PROCEEDINGS OF SCIENCE

Ultra fast variability monitoring with CTA

J. Biteau* **and B. Giebels**
Laboratoire Leprince-Ringuet, Ecole Polytechnique, CNRS/IN2P3, F-91128 Palaiseau, France
E-mail: biteau(at)in2p3.fr, berrie(at)in2p3.fr

The fast variations of flux observed at TeV energies during exceptionnal outbursts of Active Galactic Nuclei (AGN) impose strong constraints on the size and Doppler factor of the emitting region. One of the most dramatic series of TeV bursts, the giant flares of the blazar PKS 2155−304 observed by H.E.S.S. during July 2006, exhibits significant rise times as short as 3 minutes. Faster structures could not be measured because of the limited sampling rate, directly related to the sensivity of H.E.S.S.

The next generation of Atmospheric Cherenkov Telescopes, represented by the Cherenkov Telescope Array (CTA), will lower the energy threshold and increase the sensitivity in the TeV energy range. We investigate the impact of these improvements and show that a gain of almost a decade on the sampling capabilities of CTA will be achieved, allowing the probe of shorter time scales. We simulate the behaviour of PKS 2155−304 at such time scales extending the Fourier properties characterized by H.E.S.S in a first case and assuming that the source does not vary more than already observed in a second case. We show that, for each case, CTA could detect variability below the minute time scale. The consequences of such an ultra fast variability on the Doppler factor of the emitting region would challenge the models of emission of TeV blazars.

AGN Physics in the CTA Era - AGN2011,
May 16-17, 2011
Toulouse, France

*Speaker.

1. Introduction

Characteristic variability time scales of Active Galactic Nuclei (AGN) provide constraints on the properties of the emitting region. Assuming that the whole region of size R coherently emits the TeV γ rays, the causality argument yields a low bound on the minimum variability time scale t_{var} :

$$t_{var} > \frac{R}{c} \times \frac{1+z}{\delta} \tag{1.1}$$

where δ and z are the Doppler factor and redshift of the studied region. Assuming that R scales with the Schwarzschild radius $R_S = 2GM/c^2$ of the supermassive black hole, one can derive a lower limit on the Doppler factor. Such constraints have been established by Aharonian *et al.* (2007) for the exceptional outbursts of PKS 2155−304 monitored by H.E.S.S. in July 2006. To derive proper variability time scales, the lightcurve shown on Fig. 1 was fitted with a series of generalized asymetric gaussian peaks $\mathrm{I}(t) = A\exp[-(|t-t_{\max}|/\sigma_{r,d})^{\kappa}]$, where $t_{\max}$ is the time of the burst's maximum intensity A; σ_r and σ_d are the rise ($t < t_{\max}$) and decay ($t > t_{\max}$) time constants, respectively; and κ is a measure of the burst's sharpness. σ_r and σ_d being highly correlated with κ, the appropriate rise and decay times from half to maximum amplitude are then computed as $\tau_{r,d} = [\ln 2]^{1/\kappa}\sigma_{r,d}$. The peak finding and fitting procedure reveals that during MJD 59344 the flux of PKS 2155−304 is well described by a series five bursts above a constant term (see the table in Fig. 1, extracted from Aharonian *et al.*, 2007).

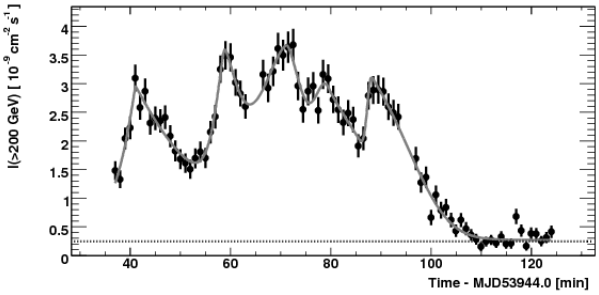

$t_{\max}$ [min]	A [10^{-9} cm^{-2} s^{-1}]	τ_r [s]	τ_d [s]	κ
41.0	2.7 ± 0.2	173 ± 28	610 ± 129	1.07 ± 0.20
58.8	2.1 ± 0.9	116 ± 53	178 ± 146	1.43 ± 0.83
71.3	3.1 ± 0.3	404 ± 219	269 ± 158	1.59 ± 0.42
79.5	2.0 ± 0.8	178 ± 55	657 ± 268	2.01 ± 0.87
88.3	1.5 ± 0.5	67 ± 44	620 ± 75	2.44 ± 0.41

Figure 1: On the left side, integral flux of PKS 2155−304 above 200 GeV during the first hours of MJD 59344. The data are binned in 1 min intervals. On the right side, results of the best χ^2 fit of the superposition of five bursts and a constant to the H.E.S.S. data. The constant term is $0.27 \pm 0.03 \times 10^{-9}\,\mathrm{cm}^{-2}\,\mathrm{s}^{-1}$ (1.1 $\mathrm{I}_{\mathrm{Crab}}$) *Extracted from Aharonian et al., 2007.*

The shortest rise time during these outbursts is $\tau_r = 67 \pm 44$ s (fifth peak) but the minute temporal binning of the time series leads to a large uncertainty on this quantity. To be conservative, Aharonian *et al.* chose the shortest significant rise time as $\tau_{r\,HESS} = 173 \pm 28$ s (first peak) and derived a lower limit on the Doppler factor $\delta > 60 - 120$, for a black hole mass ranging between $1 - 2 \times 10^9 M_{\odot}$. The variability of such an event can also be studied in the Fourier space. A structure function analysis of this lightcurve as well as the contiguous nights (Superina, 2008 - Abramowski *et al.*, 2010) shows that the Power Spectral Density (PSD) of the underlying stochastic process is well described by a power law $P_\nu \propto \nu^{-2}$, so called "red noise". The high frequency part of the spectrum is almost flat above a frequency ν_{max}, i.e. dominated by the measurement uncertainty power, which would be lowered if the flux was measured with more statistics. Thus an improvement of the

instrumental sensitivity would enable the probing of higher frequencies and bring better constraints on the shortest time scale visible in such a light curve.

2. Simulation of the lightcurves

2.1 Estimation of the flux

To estimate the flux that CTA would monitor, we first have to take into account the decrease of the energy threshold from $E_{min\ HESS} \sim 200$ GeV to $E_{min\ CTA} \sim 50$ GeV that would result in an increase of the integral flux above the threshold by a factor:

$$\Phi_{CTA}(t) = \Phi_{HESS}(t) \times \frac{\int_{E_{min\ CTA}}^{E_{max\ CTA}} F(E)\mathrm{d}E}{\int_{E_{min\ HESS}}^{E_{max\ HESS}} F(E)\mathrm{d}E} \tag{2.1}$$

where $E_{max\ HESS}$ and $E_{max\ CTA}$ are the maximum photon energies detectable by H.E.S.S. and CTA, reasonably approximated here as $+\infty$. $F(E)$, the photon spectrum - sometimes written dN/dE - is derived from the Synchrotron Self Compton (SSC) model fitted to the data of PKS 2155−304 during the 2008 multi wavelength campaign (Sanchez & Giebels, 2009 - Aharonian *et al.*, 2009). Using such a Spectral Energy Distribution, we neglect the spectral variability, taking into account only variability in the flux. $\Phi_{HESS}(t)$ is the lightcurve shown on Fig. 1, reasonably approximated by the series of bursts described in the introduction.

The energy dependency of the flux is fully accounted for in Eq. (2.1), but the modelisation of the time dependency requires knowledge on the small timescales behaviour of the flux and is thus related to the high frequency part of the PSD. If the temporal binning of the lightcurve monitored with CTA (resp. H.E.S.S.) is T_{CTA} (resp. T_{HESS}), then the highest frequency accessible for a given sampling (Nyquist frequency) will go from $\nu_{Nyq\ HESS} = 1/2T_{HESS}$ to $\nu_{Nyq\ CTA} = 1/2T_{CTA}$. The variability contained in the frequency range $[\nu_{Nyq\ HESS}, \nu_{Nyq\ CTA}]$, the extended part of the PSD, must be added to the lightcurve. Let us call the inverse Fourier transform of these extension $\Psi(t)$, then Eq. (2.1) becomes:

$$\Phi_{CTA}(t) = (\Phi_{HESS}(t) + \Psi(t)) \times \frac{\int_{E_{min\ CTA}}^{+\infty} F(E)\mathrm{d}E}{\int_{E_{min\ HESS}}^{+\infty} F(E)\mathrm{d}E} \tag{2.2}$$

To simulate $\Psi(t)$, a certain temporal behaviour must be assumed. Two cases were studied:

- First case: there is no additionnal variability above the maximum frequency for which the H.E.S.S. PSD is significantly above the measurement noise level. Then, $\Psi(t)$ represents the measurement noise fluctuations.
- Second case: the PSD is a continuous power law, even for frequencies above $\nu_{max\ HESS}$. Then $\Psi(t)$ Fourier transform is the extension of the H.E.S.S. PSD :

$$P(\nu) = \begin{cases} 0 & \text{if } \nu < \nu_{max\ HESS} \\ \\ \nu^{-2} & \text{if } \nu \geq \nu_{max\ HESS} \end{cases} \tag{2.3}$$

where $\nu_{max\ HESS} \sim 1.6 \times 10^{-3}$ Hz is the frequency for which the PSD of the HESS lightcurve is dominated by the measurement noise level. We use Timmer and König's method (1995) to

simulate light curves associated to $P(\nu)$. One of the realizations is shifted to have a null mean and finally stretched to have a proper variance. The amplitude of the stretch is determined by the Parseval's theorem: the variance of the lightcurve points equals the area below the PSD. That is to say, if the PSD is described by a power law of Fourier index α:

$$V(\Phi_{CTA}) = V(\Phi_{HESS}) \times \frac{\int_{\nu_0}^{\nu_{max\ CTA}} \nu^{-\alpha} \mathrm{d}\nu}{\int_{\nu_0}^{\nu_{max\ HESS}} \nu^{-\alpha} \mathrm{d}\nu} \tag{2.4}$$

where ν_0 is the inverse of the lightcurve duration and $\nu_{max\ CTA}$ the frequency for which the PSD of the simulated CTA lightcurve is dominated by the measurement level noise, reasonnably approximated by the associated Nyquist frequency [1].

2.2 Estimation of the error on the flux and determination of the sampling rate

The estimation of the uncertainty on the flux in each time bin is of uttermost importance since it is directly related to the sampling rate. Assuming that the number of collected photons N_γ during a time T is Poisson distributed, the error on the integrated flux is:

$$\sigma_{\Phi(>E_{min})} = \frac{\Phi(>E_{min})}{\sqrt{N_\gamma}} \tag{2.5}$$

To compute the integral flux above a threshold energy $\Phi(>E_{min})$, one has to take into account the energy dependency of the collection area, $A(E)$ obtained from simulations described by Bernlöhr (2008) / CTA consortium (2010), and weigh it by the energy distribution of the incoming photons $F(E)$:

$$\Phi(>E_{min}) = \frac{N_\gamma}{\left[\int_{E_{min}}^{+\infty} A(E)F(E)\mathrm{d}E \ / \ \int_{E_{min}}^{+\infty} F(E)\mathrm{d}E\right] \times T}. \tag{2.6}$$

Combining Eq. (2.6) and Eq. (2.5):

$$\sigma_{\Phi(>E_{min})} = \sqrt{\frac{\Phi(>E_{min})}{\left[\int_{E_{min}}^{+\infty} A(E)F(E)\mathrm{d}E \ / \ \int_{E_{min}}^{+\infty} F(E)\mathrm{d}E\right] \times T}} \tag{2.7}$$

The last missing parameter in Eq. (2.7) is the temporal binning T, which is chosen so that the mean significance of CTA lightcurve points equals the one of H.E.S.S. lightcurve points:

$$\frac{1}{N_{CTA}} \sum_{i=1}^{N_{CTA}} \frac{\sigma_{CTA}(t_i)}{\Phi_{CTA}(t_i)} = \frac{1}{N_{HESS}} \sum_{i=1}^{N_{HESS}} \frac{\sigma_{HESS}(t_i)}{\Phi_{HESS}(t_i)} \tag{2.8}$$

3. Results

The lightcurve simulated in case of no extension of the PSD is shown in Fig. 2. The increase of collection area and decrease of energy threshold allows a temporal binning of few seconds vs a minute for the H.E.S.S. lightcurve.

[1] The PSD is a steep power law, which makes the variance in $[\nu_{max\ CTA}, \nu_{Nyq\ CTA}]$ neglibible compared to the one in $[\nu_{max\ H.E.S.S.}, \nu_{max\ CTA}]$.

The analysis performed on the H.E.S.S. lightcurve by Aharonian *et al.* (2007) was applied to the CTA simulated one. This light curve was fitted with a series of bursts, detected with a peak finder, added to a constant term. The value of the latter parameter is fixed to $2.7 \times 10^{-9}\,\mathrm{cm}^{-2}\,\mathrm{s}^{-1}$, in agreement with the fit performed on H.E.S.S. data[2]. Each peak of the lightcurve shown in Fig. 2 is directly comparable to one of the H.E.S.S. lightcurve, since there is not any distortion by an additionnal variance. The resulting parameters of the fit, tabulated in Fig. 2, are thus compatible with those shown in Fig. 1. H.E.S.S. and CTA average rise/decay time resolution $\sigma_t = <\sigma_\tau\ /\ \tau>$ during the outburst can be derived from each table, yielding σ_t(H.E.S.S.)= 38% and σ_t(CTA)= 17%. This resolution improvement implies a significant measurement of the fifth peak rising time $\tau_{r\ CTA} = 60 \pm 18$ s, approximately three times smaller than $\tau_{r\ HESS} = 173 \pm 28$ s. Considering $\tau_{r\ CTA}$ as an upper limit on the variability time scale would yield a Doppler factor $\delta > 200$ - 400.

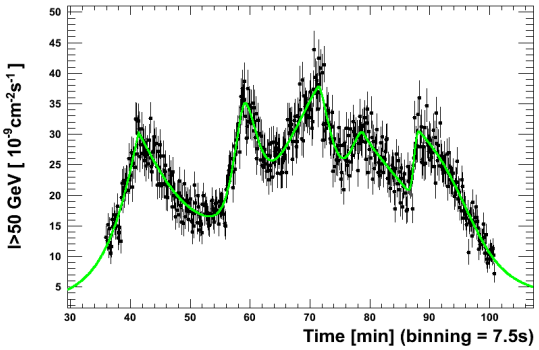

$t_{\max}$ [min]	A [$10^{-9}\,\mathrm{cm}^{-2}\,\mathrm{s}^{-1}$]	τ_r [s]	τ_d [s]	κ
41.4	26.7 ± 1.5	208 ± 13	452 ± 80	1.11 ± 0.17
59.1	16.8 ± 2.0	111 ± 14	138 ± 18	1.69 ± 0.63
71.5	32.7 ± 1.0	541 ± 106	186 ± 38	1.38 ± 0.27
78.8	23.8 ± 1.8	182 ± 36	784 ± 122	1.58 ± 0.81
< 88.3	11.9 ± 1.1	60 ± 18	513 ± 65	2.65 ± 0.40

Figure 2: On the left side, simulated integral flux of PKS 2155−304 above 50 GeV as CTA would monitor it. This simulation corresponds to the case where no additional variability is present above $\nu_{max\ HESS}$. The data are binned in 7.5 seconds intervals. On the right side, the results of the best χ^2 fit of the superposition of five bursts and a constant to the simulated CTA data. The constant term is fixed to $2.7 \times 10^{-9}\,\mathrm{cm}^{-2}\,\mathrm{s}^{-1}$

In the case where variability is added above $\nu_{max\ HESS}$, the function $\Psi(t)$ can be derived from simulations, with power above the measurement noise level up to $\nu_{max\ CTA} \sim 10^{-2}$ Hz. One of the realizations is used to obtain the simulated light curve $\Phi_{CTA}(t)$ shown in Figure 3. The addition of variance in the Fourier space yield substructures in the temporal space, the second and fourth peaks in this case, which could not have been resolved by H.E.S.S.. This particular realization peaks are clearly visible since they occur between the flares monitored by H.E.S.S.. Using the table in Fig. 1, the cumulated duration of H.E.S.S. flares can be estimated to $\sim 2/3$ of the ~ 90 minutes of observation. With respective durations of one and two minutes the additional peaks respectively have probabilities to occur between H.E.S.S. flares of $p_1 \sim 32\%$ and $p_2 \sim 30\%$, yielding a joint probability of $p_1 p_2 \sim 10\%$. Such a basic analysis show that the particular realization studied is not unlikely but the investigation of a large sample of realizations is out of the scope of this paper. The shortest significant rising time tabulated in Fig. 3, $\tau_{r\ CTA} = 25 \pm 4$ s, is approximately seven times smaller than $\tau_{r\ HESS}$, corresponding to a Doppler factor $\delta > 450 - 900$, quite unusual within the currently favored acceleration schemes (Blandford, 2005). The large Doppler factor derived would

[2] C_{CTA} and C_{HESS} being the constant terms of each light curves, we fixed $C_{CTA} = C_{HESS} \times \int_{E_{min\ CTA}}^{+\infty} F(E)\mathrm{d}E \,/\, \int_{E_{min\ HESS}}^{+\infty} F(E)\mathrm{d}E$.

certainly question the causality argument and the interpretation of such a lightcurve in terms of bursts.

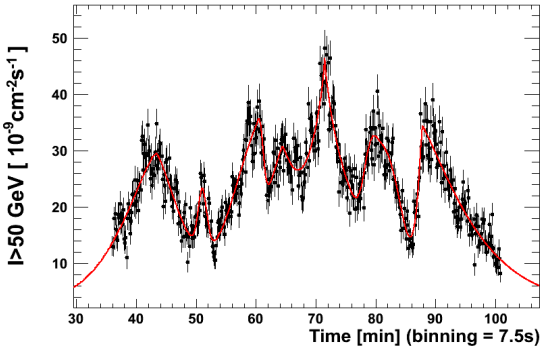

t_{max} [min]	A [$10^{-9}\,cm^{-2}\,s^{-1}$]	τ_r [s]	τ_d [s]	κ
43.3	25.7 ± 1.1	202 ± 13	147 ± 13	1.42 ± 0.15
51.0	10.9 ± 1.6	32 ± 8	34 ± 6	1.85 ± 0.44
60.4	17.5 ± 2.0	210 ± 19	37 ± 8	2.19 ± 0.35
64.4	15.1 ± 2.0	124 ± 27	60 ± 11	1.32 ± 0.28
71.5	43.7 ± 1.6	74 ± 9	80 ± 6	0.80 ± 0.11
80.5	18.3 ± 1.7	108 ± 17	177 ± 17	2.99 ± 0.43
87.8	26.8 ± 1.8	25 ± 4	235 ± 12	1.27 ± 0.10

Figure 3: On the left side, simulated integral flux of PKS 2155−304 above 50 GeV as CTA would monitor it. This simulation correspond to the case where variability is added above $\nu_{max\ HESS}$, assuming a PSD $P_\nu \propto \nu^{-2}$. The data are binned in 7.5 seconds intervals. On the right side, the results of the best χ^2 fit of the superposition of seven bursts and a constant to the simulated CTA data. The constant term is fixed to $2.7 \times 10^{-9}\,cm^{-2}\,s^{-1}$

The timing capabilities of CTA, due to its low energy threshold and large collection area, could allow to detect variations below the minute time scale. The measurement of such events will certainly raise puzzling questions on the mechanisms responsible for the TeV emission of blazars and help to unravel their mysteries.

Acknowldgements

We are very grateful to David Sanchez and Bruno Khélifi for their thoughtful remarks.

References

[1] Abramowski *et al.* (H.E.S.S. Collaboration), 2010, arXiv:1005.3702

[2] Aharonian F. *et al.* (H.E.S.S. Collaboration), 2007, ApJ 664, L71

[3] Aharonian F. *et al.* (H.E.S.S. & Fermi LAT collaborations) 2009, ApJL, 696, L150

[4] Bernlöhr K., Astropart. Phys. 30:149, 2008

[5] Blandford R.D., 2005, Probing the Physics of AGN, ASP Conference Proceedings, San Francisco, Vol. 224, 499

[6] CTA Consortium, 2010, arXiv:astro-ph/1008.3703

[7] Sanchez D. and Giebels B., 2009, arXiv:0912.5152v1

[8] Superina G., PhD thesis, Dec. 2008, Ecole Polytechnique

[9] Timmer J., König M., 1995, A&A, 300, 707